Fabrication and characterization of n-In_2S_3/p-Ag_2O/n-Si thin film, low-cost and high-efficiency photovoltaics

B.H. Hussein [a,*], H.K. Hassun [a], B. K.H. Al-Maiyaly [a], E.M-T. Salman [a]
[a] *Department of Physics, College of Education for Pure Science/Ibn Al-Haitham, University of Baghdad, 10053 Baghdad, Iraq*

Metal oxides such as Silver oxide (Ag_2O) are practically absorbed in applications thin-film solar cell due to their optimum of ban-dgap 1.6 eV and high value absorption coefficient. We propose a novel material on Ag_2O-based n-In_2S_3/p-Ag_2O/n-Si double-heterojunction solar cell, with the Cu ratios (0, 0.01, 0.02) have been proven as a successful fabric by thermal evaporation techniques as an absorbent layer. As for a single heterojunction, *p-Ag_2O/n-Si* establishes an efficiency of 1.99 %, where J_{SC} = 6.175 mA/cm^2 ;V_{OC} = 0.45 V & FF = 71.6%. Though, Ag_2O based double-heterojunction device n-In_2S_3/p-Ag_2O/n-Si with the optimized structure provides an efficiency 2.742%, J_{SC} = 7.875mA/cm^2; V_{OC} = 0.462V & FF = 75.28%. A remarkable increase of J_{SC} and V_{OC} in the double-heterojunction occurs as a result. The *n-In_2S_3/p-Ag_2O/p-Si* heterojunction causes the higher efficiency for solar cell. In the current state; efficiency conversion factor (η) increases when adding Copper and when using a window layer (n-In_2S_3), the direct transition's energy bandgap declines from 1.6 eV (when Cu is 0.0) to 1.4 eV (when Cu is 0.04) where the bandgap energy of In_2S_3 is (2 eV). The measurement for the current voltage where illumination shows that a heterojunction of a solar cell's performance is enhanced with an increase in the Cu contents. This results indicates that the preparation of the solar cells with 0.04 Cu ratios resulted in the maximum efficiency (1.99%) compared with the other prepare solar cell.

(Received September 25, 2025; Accepted December 29, 2025)

Keywords: Ag_2O Thin film, n-In_2S_3/p-Ag_2O/n-Si, double-heterojunction, Cu Doped, Photovoltaic

1. Introduction

Metal oxide semiconductor photocatalysts have become one of the biggest focuses of researches over the past few years, depending on their versatile potential in environmental purification and solar energy conversion [1] Numerous metal oxides, including Ag_2O, TiO_2, MoO_3, ZnO, ZrO_2, Fe_2O_3, WO_3, SnO_2, and $SrTiO_3$, along with certain chalcogenides such as (ZnS; CdS; WS_2, CdSe & MoS_2), have been widely studied for example photocatalyst, representing a highly active field of research [2]. Ag_2O (silver oxide) p-type semiconductor [3] shows a very small band-gap of about 1.2 to 1.5 eV, allowing it to absorber wide variety of its spectrum solar, improving its

* Corresponding author: boshra.h.h@ihcoedu.uobaghdad.edu.iq
https://doi.org/10.15251/JOR.2025.216.889

possible for application in several field [4]. The Silver oxygen (Ag,O) exists in diverse compounds,: AgO, Ag_2O, Ag_2O_3, Ag_4O_3, Ag_3O_4 & Ag_4O_4. Ag_2O is the most thermodynamically steady of these oxides [5]. Simple cubic structure at RT [6]. Countless production methods have been applied to produce Ag2O nanoparticles, including hydrothermal precipitation [7], sol-gel[8] Microwave-assisted techniques[9]. and solvo-thermal [10]. pulsed laser deposition [11] RTO technique using halogen lamp [12] DC magnetron sputtering [13] Silver oxide (Ag_2O) is a semiconductor with a bandgap between 1.2 and 3.4 eV on R.T, varying based on its stoichiometric composition [14] The employment of window layer (In_2S_3) can too decreasing the toxic countryside by replace the CdS and CdTe layers used in solar cells [15]. In_2S_3 has garnered significant consideration due to its optical transparency, stability in thermal & wide band energy gap 2–2.9 eV. dependent on the process of the preparation of In_2S_3 [16]. It is capable of existing in three distinct crystalline forms, depending on the temperature: defective spinel (β-In_2S_3), defective cubic (α-In_2S_3); and layer structure (γ-In_2S_3). The β-In_2S_3 at room temperature of these phases exhibits the highest stability [17]. n-type semiconductor (In_2S_3) [18,19]. In this research, it was found that the doping of Copper (Cu) in Ag_2O takes up the cation (In this case is Ag) site, instead of anion (Which in this case is O) site, subsequently, the relatively low electronegativity of Cu (1.9) in comparison to those of Ag atoms (1.93) or O atoms (3.44), the anticipation of a major creation in the di- valence Cu Ag 2+ treats that performance as per an active donor. Ionic radius is the main factor used to decide what to choose from the applicable contribution materials [20]. Optical, structural, & electrical properties of Ag_2O films could be tuned—for instance, through the doping with Cu, whose ionic radius is smaller than that of Ag and O ions. Cu is a decent dopant for the Ag_2O lattice as a result of the lower ionic radii Cu+2 (0.71Å) compared to that of Ag +2 (1.08Å), O-1 (1.27Å) [20,21]. To distinguish Ag_2O-based device of photovoltaic, it is important to understand affection of (WL) on the heterojunction structures' absorber layer. In this research the manufacture of a double-heterojunction high-efficiency, low-cost, and environmentally friendly thin films solar cell by n-In2S3/p-Ag2O/n-Si, where Ag_2O (low bandgap) with In_2S_3 (wide bandgap) for broad-spectrum absorption with many Copper ratios (0, 0.02, 0.04) for the solar cells devices were produced by the help of vacuum evaporation technique.

2. Experimental

As for the research, Ag_2O based dual-heterojunction solar cell has been planned using indium sulfide (In_2S_3) by way of a window layers when a thickness of (100 nm), dual-heterojunction structures of n-In_2S_3/p-Ag_2O/n-Si, the p-Ag_2O: Cu by way of a layer of absorption when the thickness of thin film being around 500 nm, based on the following schematic diagram which is designed n-In2S3/p-Ag_2O /n-Si PV cells of heterojunction have been shown as in the Figure (1). High-purity silver oxide (Ag_2O) thin films were deposited on both n-type single-crystal Si wafers with (111) orientation, an indirect bandgap of 1.1 eV, (500 nm thickness) for photovoltaic applications, as well as on glass substrates to study the electrical, structural; and optical properties. Ag_2O films were subsequently formed via thermal oxidation at 750 K under an ambient oxygen flow rate of 500 sccm for two hours. Then, the films were doped with different concentrations of pure copper (Cu: 0, 0.1, 0.2 at.%) using thermal diffusion at 473 K for one hour. The film thickness was measured using an optical interferometer method. An In_2S_3 alloy was produced from a stoichiometric

(2:3) weighed mixture of high-purity (99.99%) indium and sulfide. Mixed elements were fused in cleaned, 22 cm-long quartz ampules under a pressure of 6×10^{-3} mbar. After being heated at 1173 K for six hours in an electric oven, the ampules were cooled to (R.T). A thin film of In_2S_3 A thin deposited by vacuum thermal evaporation with thicknesses 100 nm as window layers.

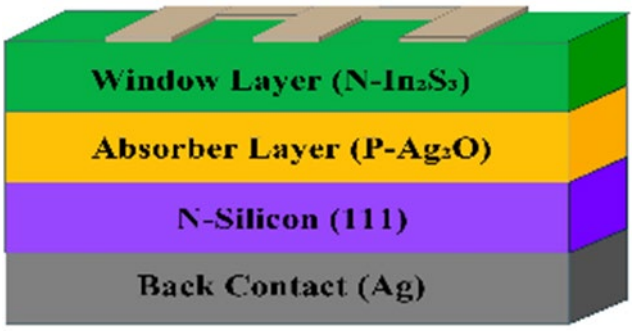

Fig. 1. The diagram of a Schematic block of n-In2S3/p-Ag2O/n-Si dual heterojunction solar cell

The synthesized *Ag_2O and In_2S_3* properties were characterized by means of XRD and FESEM. Structure of these film was examined using Scherer's Formula was employed to calculate their crystalline properties [22-23]:

$$C.S = \frac{0.9 * \lambda}{\beta \cos\theta} \tag{1}$$

β denotes the width of the peak at half diffraction maximum, crystallite size (C.S), (θ) is the diffraction peak angle. Formula for crystal plane spacing in cubic crystalline phase structure [24]. The To determine the energy gap, Measurements of optical transmission within the 400–1000 nm wavelength rang were performed. The optical characteristics of the thin film preparation have been observed through transmission and absorption spectra spanning a wavelength range of 400 to 1000 nanometers. The energy gap (Egopt) has been calculated from the absorption spectrum using the Tauc equations and, Lambert's law, respectively [25-27]:

$$\alpha = \frac{2.303\ A}{t} \tag{2}$$

$$\alpha h\upsilon = D\ (h\upsilon - E_g^{opt})^r \tag{3}$$

Absorption coefficient is signified by (α). The exact values of the temperature-dependent constant (D) and (hυ) signify the magnitude of the photons' incident energy, while the factor r specifies dependence on optical transition type and t thickness.

The predominant carrier concentrations were determined using a Van-der Pauw system (Ecopia HMS 3000) [28], the type of carriers in Ag_2O and In_2S_3 film, and mobility carrier from Hall effect. We calculated current-voltage (I-V) features by applying the Shockley equation

$$I = I_s\left\{\exp\left(\frac{eV}{\beta k_B T}\right) - 1\right\} - I_L \tag{4}$$

The fill factors are the ratios between the (maximum power) in the solar cell (P_{max}) & multiply of I_{sc} & V_{oc}. By the means of the following relation [26]:

$$\text{Fill Factor (F.F)} = \frac{P_{max}}{V_{oc}J_{sc}} = \frac{V_{max}I_{max}}{V_{oc}I_{sc}} \quad (5)$$

where V_{max} and I_{max} are the voltage and the current of the P_{max}.

Finally, The solar cell's efficiency conversion factor (η) was calculated using the following formula [29]:

$$\eta = \frac{P_{max}}{P_{in}} * 100\% \ \frac{F.F \times J_{sc} \times V_{oc}}{P_{in}} \times 100\% \quad (6)$$

The symbols (V_{oc}); (J_{sc}); and $(F.F)$ represent the open-circuit voltage short circuit current density; & fill factor, respectively. Pindenotes input power, which is 100 (mWcm-²)

3. Result and Discussion

Figure 2a shows XRD graphs of the synthesized Ag_2O. All samples showed as good and polycrystalline. The peak positions of the crystallite had been observed at the documenting of XRD from (20° to 80°) angle. Note that at 38.3°, 50.37°, and 66.78° they belong to the corresponding planes of (101), (102), and (103), respectively. These planes were confirmed utilizing the ICDD 00-019-1155 card. The samples' crystalline sizes were calculated using the equation of Scherer (1) and the results are shown in Table 1a. As for the copper ratio increases, the crystalline size also increases. We can notice that when adding the Cu ratios (0.02, 0.04) "the peaks in the diffraction pattern shift to lower angles, and the intensities peaks mostly increase as the doping and crystallite size become larger, and this be contingent on ion size differences among Ag, copper and the increase in intensity refers to the include of the Copper atom in the Ag vacancies progress for the crystallinity growth. The crystallite size of the Ag_2O: 0.04 Cu has high crystallite size from other films due to the relatively small size of atom (the ionic radius for Cu 0.71Å) [20,21] doping enters the atoms diffuses through the lattice of structure and moves into Interstice's position within the Ag_2O. It is known that the effective doping effect of in semiconductors occurs when the ionic diameter of the doping atoms is smaller or equal to the host material. Figure 2b displays the XRD pattern for In_2S_3 thin film where thickness 100 nanometers. Figure X shows that the In_2S_3 thin film are polycrystalline with a stable tetragonal β-In_2S_3 structure and a preferred (109) orientations at ($2\theta \approx 27.35°$), which agree with the findings of [18]. The Table 1b shows excellent agreement between the experimental values and the ICDD standard (00-025-0390).

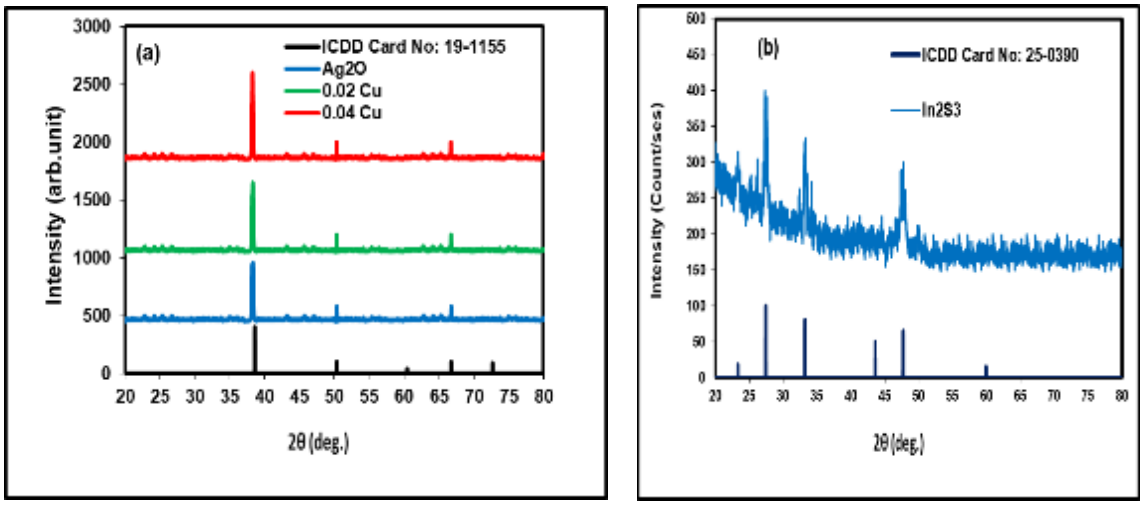

Fig. 2. XRD for (a) Ag_2O thin film at Cu (0.0, 0.02, & 0.04). & (b) In_2S_3 thin film.

Table 1a. X-ray diffraction for the Ag_2O thin films with Cu (0.0, 0.02, & 0.04).

Copper ratio	hkl	d Å Std.	d Å Exp.	2θ Deg. Std.	2θ Deg. Exp.	β Deg.	C.S nm
Ag_2O (0.0 Cu)	**(101)**	2.33	2.347	38.6	38.3	0.204	43.06
	(102)	1.81	1.80	50.37	50.37		
	(103)	1.4	1.399	66.76	66.78		
Ag_2O (0.02 Cu)	**(101)**	2.33	2.347	38.6	38.3	0.198	44.36
	(102)	1.81	1.81	50.37	50.34		
	(103)	1.4	1.399	66.76	66.74		
Ag_2O (0.04 Cu)	**(101)**	2.33	2.349	38.6	38.26	0.186	47.22
	(102)	1.81	1.811	50.37	50.32		
	(103)	1.4	1.400	66.76	66.72		

Table 1b. X-ray diffraction of In2S3 thin films.

Thin film	hkl	dÅ Std.	dÅ Exp.	2θ (Deg.) Std.	2θ Deg. Exp.	β Deg.	C.S nm
In_2S_3	**(109)**	3.24	3.25	27.429	27.35	0.6	20.81
	(0012)	2.69	2.69	33.228	33.2		
	(2212)	1.905	1.904	47.7	47.699		

The FESEM images illustrate how Cu doping modifies Ag_2O microstructure in Figure 3. While a lower ratio of doping results in more understated changes that may influence the material's optical, electronic properties, higher ratio of doping products more pronounced structural and morphological changes. These perceptions are very useful for photovoltaic applications. The pure

Ag_2O image most likely depicts homogeneous particles with a constant size distribution, perhaps spherical or cubic in shape. Lattice strain or defects may result from the Cu 0.02 doping, changing the surface texture without significantly altering the overall morphology. As the Cu doping ratio increased, the structural and morphological changes became more evident. Higher Cu ratios (0.04) may promote particle aggregation or clustering due to altered surface energies.

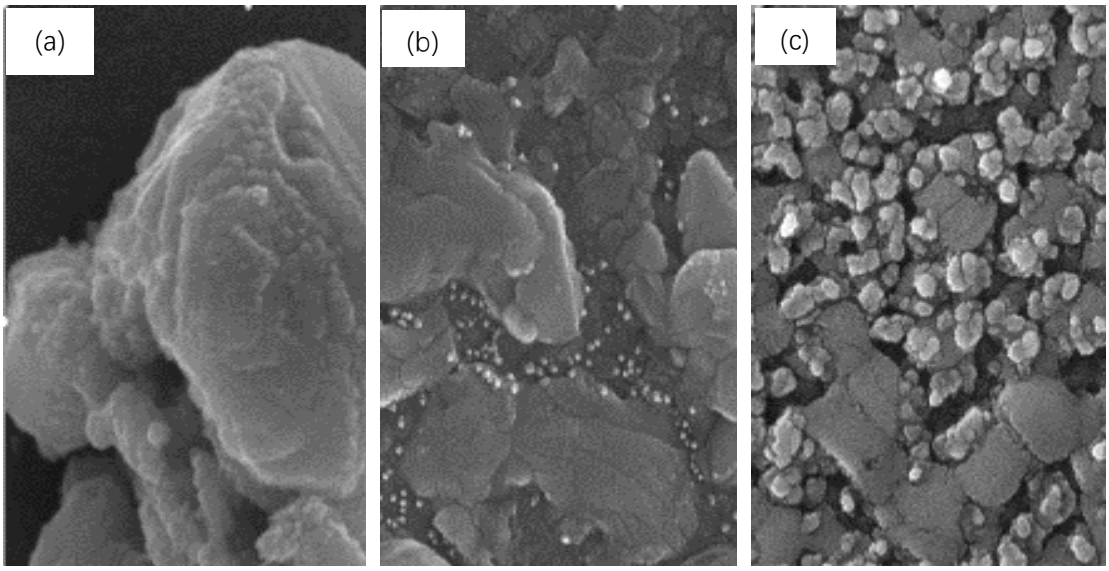

Fig. 3. FESEM micrograph of Ag2O thin film with Cu (0.0, 0.02, and 0.04).

Figure (4a) shows the Copper ratios' effects on the absorption Spectra of the Ag_2O film. It has been observed that the thin films absorption happens to increase with a gradual decrease in the wavelength. This might have occurred because of the decrease in the corresponding transmittance with a gradual decrease in the wave-length as displayed in Figure (4a). Optical absorbance obviously exhibits a band edge displacement as a result of addition of copper in the range of visibility 300-650 nm. Therefore, the films are decent application as an absorption layer in the solar cells due to the high absorption within the visible region. By examining optical characteristics for In_2S_3 via RT, we have successfully produced a transmittance spectrum of In_2S_3 thin film when a wave-length range (300-1000) nm. The Figure (4b) shows those spectra, in which they display a decrease in transmittance values upon decreasing these wavelengths. The transmittance high value only means that it is a decent for window material layer in multi-layers solar cell as in the study [30]. he optical gap energy was strongminded from a Taucs plots [26]. The variation of Eg with Ag_2O and different Cu ratios (0.02, and 0.04). is further demonstrated in the Figure (5a). The direct transition (allowed) energy gap of (Ag_2O) film was to compute to 1.6 eV in good agreement with [4] The value decreases from approximately 1.6 eV in the undoped state to a minimum of 1.4 eV at a copper ratio of 0.04, this means it has been decreased after doping as the result of adding the Copper dopant atoms lead to increase of crystallites size and the more absorbance is possible to get in Ag_2O: 0.04 Cu films Copper doping shifted the band-gap of Ag_2O film closer to valence band edge, alongside the direct transition as in Table 2. Gap energy value for In_2S_3 as a window layers is (2 eV) [16] as in Figure (5b).

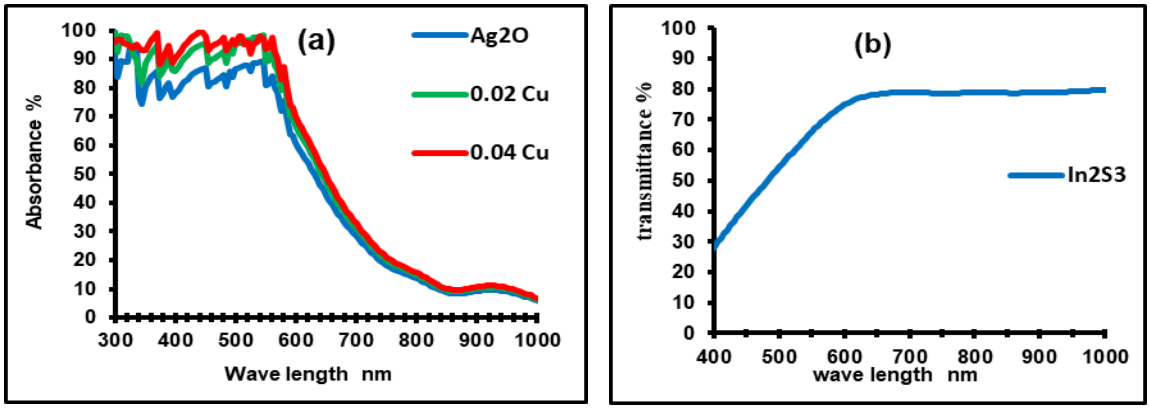

Fig. 4. (a) The absorbance Ag_2O thin films with Cu (0.0, 0.02, and 0.04). (b) transmittance vs. wavelength for In_2S_3 thin film.

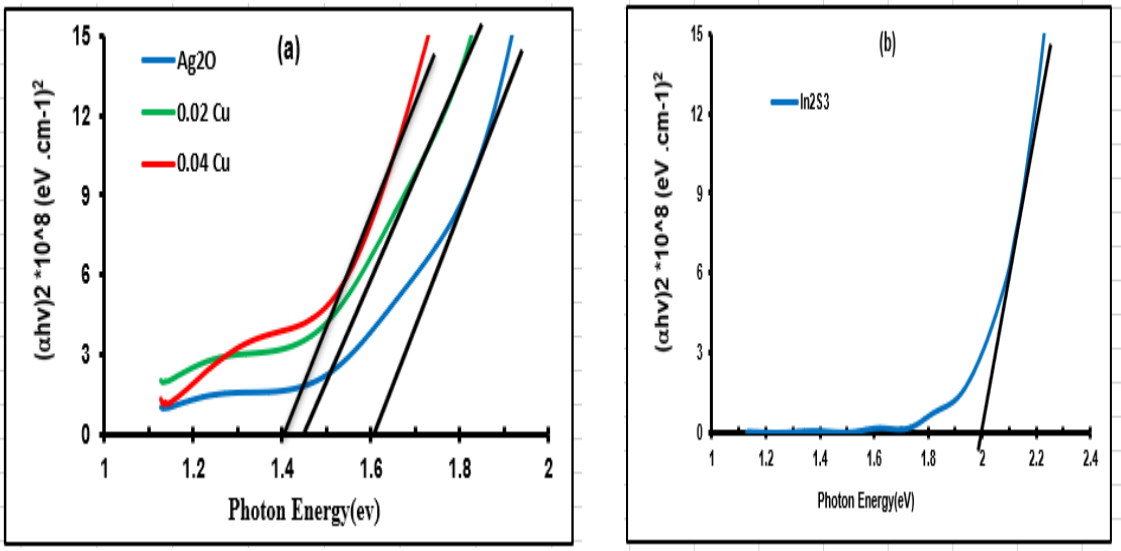

Fig. 5. $(\alpha h\upsilon)^2$ vs. photon energy for (a) Ag_2O thin films with Cu (0.0, 0.02, and 0.04). (b) for In_2S_3 thin film.

Table 2. The optical band-gap of Ag_2O thin film at Cu (0.0, 0.02 & 0.04).

Copper ratios	E_g^{opt} (eV)
Ag_2O (0.0 Cu)	1.6
Ag_2O (0.02 Cu)	1.45
Ag_2O (0.04 Cu)	1.4

Ag_2O is based on a dual-heterojunction solar device designed using In_2S_3 semiconductor as n-type, where sulfur vacancy acts as a donor state that free electrons. Because of this property, it has been considered a promising window layer for photovoltaic devices [18,19]. To fabricate the

heterojunction, the semiconductor type (p-type and n-type) of the thin films must be determined. The Hall coefficient (R_H) and mobility (μH) were used to identify the major charge carrier type and its mobility for Ag_2O thin film with changing copper (Cu) doping concentrations. Silver oxide (Ag_2O) is inherently a p-type semiconductor because its dominant defects (silver vacancies) introduce mobile holes as the primary charge carriers. The data in the Table 3 & Figure 6 indicate that Hall-coefficient of Ag_2O thin film reduces the carrier's concentration. his points to lower resistivity (ρ) and higher conductivity (σ) for thin layers. It can be seen that the resistivity of Cu doped Ag_2O thin film is much lower than that of pure thin film as a result of free hole release from the substitution for doped ions or atom at these sites, which are employed by Ag ions. A peak NH concentration of 6.12×10^{17} cm^{-3} was recorded at a copper content (Cu) of 0.04 at R.T.

Table 3. The electric data of Ag_2O thin film where Cu (0.0, 0.02, & 0.04).

Copper ratios	R_H cm^3C^{-1}	N_A*10^{17} $(1/cm^3)$	μ_H $cm^2/V.s$	ρ Ω.cm
Ag2O (0.0 Cu)	10.77586	5.8	11.85345	0.909091
Ag2O (0.02 Cu)	10.5042	5.95	12.07983	0.869565
Ag2O (0.04 Cu)	10.21242	6.12	12.2549	0.833333

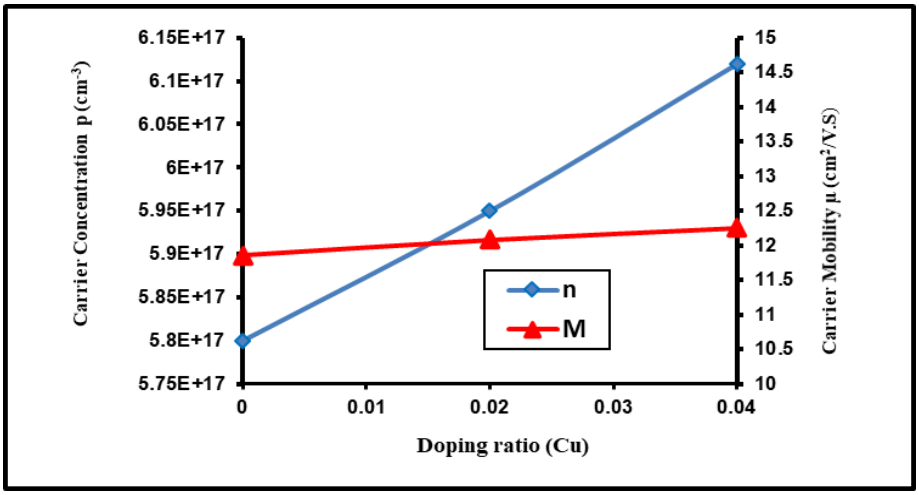

Fig. 6. Carrier concentration and Mobility for Ag_2O thin films with Cu (0.0, 0.02, and 0.04).

The PV performance of Ag_2O solar cell by altering the Cu doping from 0.02 to 0.04 of the Ag_2O absorber layer. The variation of Cu doping caused a significant change in V_{OC} as well as the corresponding efficiency as shown in Figure 7. The reduction in recombination current enhances the V_{OC} of the solar cell [31]. The J_{SC} increases slightly with the enhancement in Cu doping and FF increases with doping. Therefore, the improvement of V_{OC} and FF improves the efficiency from 1.99% to 2.742%. Figure 7 and *Table 4* represent that the proposed cell's efficiency fully depends upon the gradual addition of Cu doping. Efficiency can be achieved with the Cu doping more than 0.02.

The Ag_2O absorber for example, Cu doping equal to 0.02 is not powerful enough to make the use of all of the photons that fall on the cell. When the Cu doping is increased in the cells, the amount of current during exposure to sunlight improves.

The impact of In_2S_3 window layer on the PV output for Ag_2O thin film solar device was investigated. In_2S_3 has a wide bandgap (2.0 eV), making it an excellent window layer that allows high transmission of sunlight to the absorber layer (Ag_2O). Since Ag_2O has a narrower bandgap (1.6–1.4 eV), the In_2S_3 layer ensures minimal parasitic absorption, maximizing photon absorption in the active layer, In_2S_3 forms a favourable heterojunction with Ag_2O, improving charge separation and reducing recombination. Its high electron mobility facilitates efficient electron extraction, increasing the short-circuit current (Jsc). The conduction band offset between In_2S_3 and Ag_2O promotes electron flow while blocking holes, reducing interfacial recombination. A properly optimized In_2S_3 layer can passivate defects at the interface, improving the open-circuit voltage (Voc). In_2S_3 is chemically stable and less prone to oxidation compared to CdS (a traditional window layer), enhancing the long term stability for Ag_2O-solar cell.

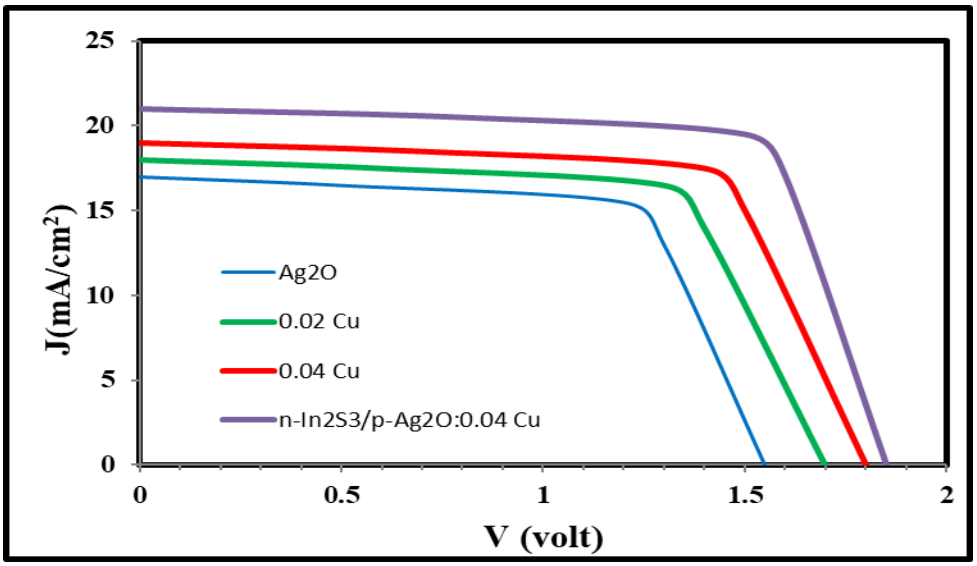

Fig. 7. I-V of heterojunction p-Ag_2O/n-Si at Cu 0.0, 0.02, & 0.04 and n-In_2S_3/ p-Ag_2O (0.04 Cu)/n-Si.

Table 4. I-V features of the heterojunction p- Ag_2O/n-Si by Cu 0.0, 0.02, & 0.04 and n-In_2S_3/p-Ag_2O (0.04 Cu)/n-Si.

Parameter	*Ag_2O (0.0 Cu)*/Si	*Ag_2O (0.02 Cu)/Si*	*Ag_2O (0.04 Cu)/Si*	*In_2S_3/Ag_2O (0.04 Cu)/Si*
V_{oc} Volt	0.3875	0.425	0.45	0.4625
J_{sc} mA/cm^2	5.1	5.85	6.175	7.875
V_m Volt	0.3	0.325	0.35	0.375
J_m mAcm-^{2}	4.65	5.3625	5.8675	7.3125
F.F	0.705	0.7009	0.716	0.752
Efficiency %	1.395	1.742	1.99	2.742

4. Conclusions

In this study, a novel double-heterojunction solar cell structure, n-In_2S_3/p-Ag_2O/n-Si, with varying Cu doping ratios (0, 0.02, 0.04) in the Ag_2O absorber layer, was successfully fabricated using the thermal evaporation method. The incorporation of Cu doping and the use of In_2S_3 as a window layer significantly enhanced the photovoltaic performance of the device. These results highlight the potential of Cu-doped Ag_2O and In_2S_3 in double-heterojunction solar cells, offering a promising pathway for the development of efficient and environmentally friendly photovoltaic devices.

Availability of Data and Materials

The Corresponding author can provide data upon reasonable request.

Author Contributions

The authors confirm contribution to the paper in the execution of the examination, the administration of the data and the writing of the manuscript.

Acknowledgment

The authors would like to thank the Thin Film Lab., Department of Physics, College of Education for Pure Science /Ibn Al-Haitham, University of Baghdad.

Funding

The authors have not disclosed any fundings.

Conflict of Interest

The authors declare no conflicts of interest to report regarding the present study.

References

[1] W. M. Shume, H. C. A. Murthy, E. A. Zereffa.Journal of Chemistry. 5039479. 1-15 (2020). https://doi.org/10.1155/2020/5039479

[2] J. Cao, B. Luo, H. Lin, S. Chen. Journal of Hazardous Materials. **190**(1–3). 700–706(2011). https://doi.org/10.1016/j.jhazmat.2011.03.112

[3] A. S. Gungure, L. T. Jule, N. Nagaprasad, K. Ramaswamy, Scientific Reports. **14**. 26967. (2024). https://doi.org/10.1038/s41598-024-75614-8
[4] S. Muhammad, A. Ali, S. Zahoor, X. Xinghua, J. Shah, M. Hamza, M. Kashif, S. Khan, B. K. A. Khel, A. Iqbal. Acta Scientific Applied Physics. **3**(7). 33-48(2023).
[5] J. F. Pierson, C. Rousselot. Surface and Coatings Technology. **200**(1-4). 276-279(2005). https://doi.org/10.1016/j.surfcoat.2005.02.005
[6] A. Hammad, H. Abdel-Wahab, M. SH. A. ALshahrie. Digest Journal of Nanomaterials and Biostructures. **11**(4). 1245-1252(2016).
[7] M. I. Rahmah, N, M. Saadoon, A. J. Mohasen, R. Ihssan, T. A. Fayad, N. M. Ibrahim. Journal of the Mechanical Behavior of Materials. **30**(1). 207-212(2021).
[8] D. R. Eddy, M. D. Permana, K. Sakti, D. Dwiyanti, T. Takei, N. Kumada, I. Rahayu. Emergent Materials. **6**(4). 1231-1242(2023).
[9] J. Fowsiya, G. Madhumitha. Journal of Cluster Science, **30**(5). 1243-1252(2019).
[10] K. Maesaroh, M. D. Permana, D. R. Eddy, I. Rahayu. Trends in Sciences. **20**(3). 4350-4350(2023). https://doi.org/10.48048/tis.
[11] N. M .Abas, A. A. Baqer. Baghdad Science Journal. **21**(4). 1391-1402(2024).
[12] R. A. Ismail, K. Z. Yahya, O. A. Abdulrazaq. Surface Review and Letters. **12**(2). 299–303 (2005). https://doi.org/10.1142/S0218625X05007074
[13] F. Hajakbari, M. Ensandoust. Acta Physica Polonica A. **129**(4). 680-682(2016).
[14] R. A. Ismail, A. E. Al-Samarai, F. M. Ahmed. Optik. **257**. 168794. (2022). https://doi.org/10.1016/j.ijleo.2022.168794
[15] P. E. Rodríguez-Hernández, J. G. Quiñones-Galván, L. Marasamy, M. Morales-Luna, J. Santos-Cruz, J. S. Arias-Cerón, O. Zelaya-Angel, F. Moure-Floresde. Materials Science in Semiconductor Processing. **103**(15). 104600. (2019).
[16] S. Thierno, H. Bouchaib, M. Bernabe, M. Mollar, L. Larbi, F. Mounir. In International Renewable and Sustainable Energy Conference (IRSEC). 58-62(2013).
[17] D. Alagarasan, S. S. Hegde, R. Naik, P. Murahari, H. D. Shetty, F. H. Alkallas, A. B. Gouider Trabelsi, F. S. Khan, S. AlFaify, M. Shkir. Journal of Photochemistry and Photobiology A: Chemistry. **454**(1). 115697. (2024). https://doi.org/10.1016/j.jphotochem.2024.115697
[18] N. Akcay, B. Erenler, Y. OZEN, V. F. GREMENOK, K. P. Buskis, S. OZCELIK. Gazy University Joural of Science. **36** (3). 1351-1367(2023). https://doi.org/10.35378/gujs.1075405
[19] P. P. Atre, M. A. Desai, A. N. Vyas, S. D. Sartale, B. N. Pawar. ES Energy and Environment. **12**. 52-59(2021). https://dx.doi.org/10.30919/esee8c1041
[20] R. D. Shannon. Foundations and Advances **32**(5). 751-767(1976).
[21] N. N. Greenwood, A. Earnshaw. University of Leeds, U.K. 9780080501093. (2012).
[22] S. N. Sobhi, B. H. Hussein. Ibn AL-Haitham Journal For Pure and Applied Sciences. **35**(3). 16-24(2022). https://doi.org/10.30526/35.3.2824
[23] R. H. Athab, B. H. Hussein. Chalcogenide Letter. **20**(7). 477 - 485(2023). https://doi.org/10.15251/CL.2023.207.477
[24] S. N. Sobhi, B. H. Hussein. Journal of Ovonic Research. **18**(4). 519 – 526(2022). https://doi.org/10.15251/JOR.2022.184.519
[25] S. N. Sobhi, B. H. Hussein. Chalcogenide Letters, **19**(6). 409 – 416(2022). https://doi.org/10.15251/CL.2022.196.409
[26] S. M. Ali, H. K.Hassun, A. A. Salih, R. H. Athab, B. K. H. Al-Maiyaly, B. H. Hussein.

Chalcogenide Letters. **19**(10). 663 – 671(2022). https://doi.org/10.15251/CL.2022.1910.663
[27] B. K. Al-Maiyaly, B. H. Hussein, A. A. Salih, A. H. Shaban, S. H. Mahdi, I. H. Khudayer. AIP Conference. Proceedings. **1968**(1). 030046-1–030046-11(2018). https://doi.org/10.1063/1.5039233
[28] M. R. Jobayr, E. M-T. Salman. Journal of Semiconductors. **44**(3). 1-9(2023). https://doi.org/10.1088/1674-4926/44/3/032001
[29] R. H. Athab, B. H. Hussein. Chalcogenide Letter, **20**(2). 91-100(2023). https://doi.org/10.15251/CL.2023.202.91
[30] E. Alamoudi, A. Timoumi. Results in Physics. **40**. 105858. (2022). https://doi.org/10.1016/j.rinp.2022.105858
[31] S. K. Mostaque, B. K. Mondal, J. Hossain. Materials Today Communications. **33**. 104442. (2022). https://doi.org/10.1016/j.mtcomm.2022.104442